Longitudinal MicroRNA Signature of Conversion to Psychosis

Anton Iftimovici, Qin He, Chuan Jiao, Edouard Duchesnay, Marie-Odile Krebs, Oussama Kebir, Boris Chaumette

▶ **To cite this version:**

Anton Iftimovici, Qin He, Chuan Jiao, Edouard Duchesnay, Marie-Odile Krebs, et al.. Longitudinal MicroRNA Signature of Conversion to Psychosis. Schizophrenia Bulletin, 2023, 50 (2), pp.363-373. 10.1093/schbul/sbad080 . inserm-04187662

HAL Id: inserm-04187662

https://inserm.hal.science/inserm-04187662v1

Submitted on 25 Aug 2023

HAL is a multi-disciplinary open access archive for the deposit and dissemination of scientific research documents, whether they are published or not. The documents may come from teaching and research institutions in France or abroad, or from public or private research centers.

L'archive ouverte pluridisciplinaire **HAL**, est destinée au dépôt et à la diffusion de documents scientifiques de niveau recherche, publiés ou non, émanant des établissements d'enseignement et de recherche français ou étrangers, des laboratoires publics ou privés.

Copyright

Longitudinal microRNA signature of conversion to psychosis.

[Published as: Iftimovici A, He Q, Jiao C, Duchesnay E, Krebs MO, Kebir O, Chaumette B. Longitudinal MicroRNA Signature of Conversion to Psychosis. Schizophr Bull. 2023 Aug 22:sbad080. doi: 10.1093/schbul/sbad080. PMID: 37607340.]

Authors: Anton Iftimovici[1,2], Qin He[1], Chuan Jiao[1], Edouard Duchesnay[2], Marie-Odile Krebs[1,3], Oussama Kebir[1,3], Boris Chaumette[*,1,3,4]

[1] Université de Paris, Institute of Psychiatry and Neuroscience of Paris (IPNP), INSERM U1266, GDR 3557-Institut de Psychiatrie, Paris, France

[2] NeuroSpin, Atomic Energy Commission, Gif-sur Yvette, France

[3] GHU Paris Psychiatrie et Neurosciences, Paris, France

[4] Department of Psychiatry, McGill University, Montréal, Québec, Canada.

*** To whom correspondence should be addressed:**

Boris Chaumette - ORCID: 0000-0002-1313-2788, Email: boris.chaumette@inserm.fr

Address: INSERM U1266 - 108 rue de la Santé - F-75014 Paris - France

Phone: +33140789219

Abstract word count: 225

Text word count: 3993

Abstract

Background and Hypothesis : The emergence of psychosis in ultra-high-risk subjects (UHR) is influenced by gene-environment interactions that rely on epigenetic mechanisms such as microRNAs. However, whether they can be relevant pathophysiological biomarkers of psychosis' onset remains unknown.

Study Design : We present a longitudinal study of microRNA expression, measured in plasma by high-throughput sequencing at baseline and follow-up, in a prospective cohort of 81 UHR, 35 of whom developed psychosis at follow-up (converters). We combined supervised machine-learning and differential graph analysis to assess the relative weighted contribution of each microRNA variation to the difference in outcome and identify outcome-specific networks. We then applied univariate models to the resulting microRNA variations common to both strategies, to interpret them as a function of demographic and clinical covariates.

Study Results : We identified 207 microRNA variations that significantly contributed to the classification. The differential network analysis found 276 network-specific correlations of microRNA variations. The combination of both strategies identified 25 microRNAs, whose gene targets were overrepresented in cognition and schizophrenia GWAS findings. Interpretable univariate models further supported the relevance of miR-150-5p and miR-3191-5p variations in psychosis onset, independent of age, sex, cannabis use, and medication.

Conclusions : In this first longitudinal study of microRNA variation during conversion to psychosis, we combined two methodologically independent data-driven strategies to identify a dynamic epigenetic signature of the emergence of psychosis that is pathophysiologically relevant.

Introduction

Psychosis is a frequent and disabling disorder that occurs during adolescence and early adulthood.[1] Subjects at ultra-high-risk for psychosis (UHR) can be routinely screened in clinical practice,[2] but while 25% of UHR individuals will convert to psychosis at three years,[3] outcome remains difficult to predict, and reliable biomarkers are needed to improve early healthcare. The emergence of psychosis involves progressive interactions between genetic vulnerability and environmental pressure,[4,5] which may depend on epigenetic factors.[6–11] Among such mechanisms, microRNAs are increasingly studied as potential biomarkers.[8] They are short non-coding RNAs, about 19-22 nucleotides long, which regulate translation of messenger RNAs (mRNAs).[12] Many were found differentially expressed in schizophrenia,[7,13] and schizophrenia-risk genes are highly regulated by microRNAs.[14] Most of the deregulated neurotransmitter systems in schizophrenia also depend on specific microRNA regulations.[15] One of the most replicated microRNAs associated with schizophrenia, miR-137, has thus been shown to regulate AMPA and metabotropic glutamate receptors crucial for synaptic plasticity.[16] Other microRNAs target D2 and D3 dopamine receptors and their dysfunction is associated with schizophrenia-like phenotypes in both humans and animal models, where their rescue improves behavioral measures.[17,18] MicroRNAs networks were also shown to regulate GABAergic pathways through their effect on *GAD-1* and *VGAT* expression in mice models.[19]

However, the diagnostic relevance of microRNAs remains largely unknown. Only longitudinal studies may provide insight into whether specific microRNAs could be markers of trait or of state. The differential expression of certain microRNAs, in subjects with schizophrenia compared to controls, could for instance be stable over time, independently of clinical improvement[20] or treatment.[21] Conversely, other microRNA variations could relate to medication and reflect treatment response,[22] or correlate with symptomatology improvement.[23] In the UHR population, it has been suggested that baseline microRNA measures in peripheral blood could help to classify between converters and non-converters to psychosis.[11] Nevertheless, it is unclear whether such baseline measures are stable markers of trait, or state-dependent markers that vary across time. Unlike cross-sectional designs, longitudinal studies during conversion to psychosis may detect such dynamic biomarkers, more relevant to distinguish between pathophysiological trajectories.[24]

To this purpose, we measured microRNA variation (Δmirna) between baseline and one-year follow-up in a prospective UHR cohort of 81 subjects, and compared subjects who converted to psychosis to those who did not. We present here a combination of two data-driven strategies leveraging all sequenced microRNAs to account for the fact that pathophysiological processes may be mediated by small changes in a co-regulatory network of highly interconnected microRNA variations,[25] especially as brain-enriched microRNAs share common mRNA targets resulting in cooperative repression.[26] First, we used a Δmirna-based supervised classifier to identify cooperative Δmirnas with a joint effect on psychosis. Secondly, a network analysis highlighted Δmirna-Δmirna interactions that were specific to conversion to psychosis. The pathophysiological relevance of Δmirnas overlapping between these strategies was then assessed by an enrichment study of their targets in disease-related GWAS, and gene and disease ontologies. Finally, a univariate analysis of the resulting Δmirnas as a function of demographic and clinical covariates provided a *forward* interpretable model of the previous *backward* data-driven solutions (**Figure 1**).[27] Overall, we make the hypothesis that a combination of Δmirna may be a longitudinal signature of conversion to psychosis.

Figure 1 - **Methodological pipeline:** combination of two data-driven strategies leveraging all sequenced microRNAs at two timepoints, before and after conversion to psychosis. The variation of microRNA across time, Δmirna, was used as input. A Δmirna-based supervised classifier identified cooperative Δmirnas with a joint effect on psychosis. Δmirna-Δmirna interactions specific to conversion to psychosis were identified through network analysis. The common Δmirna resulting from both methods were then used to predict their gene targets, on which the pathway analysis was performed. FInally, a univariate analysis of the resulting Δmirnas as a function of demographic and clinical covariates checked for the association between these microRNAs and outcome in an interpretable model.

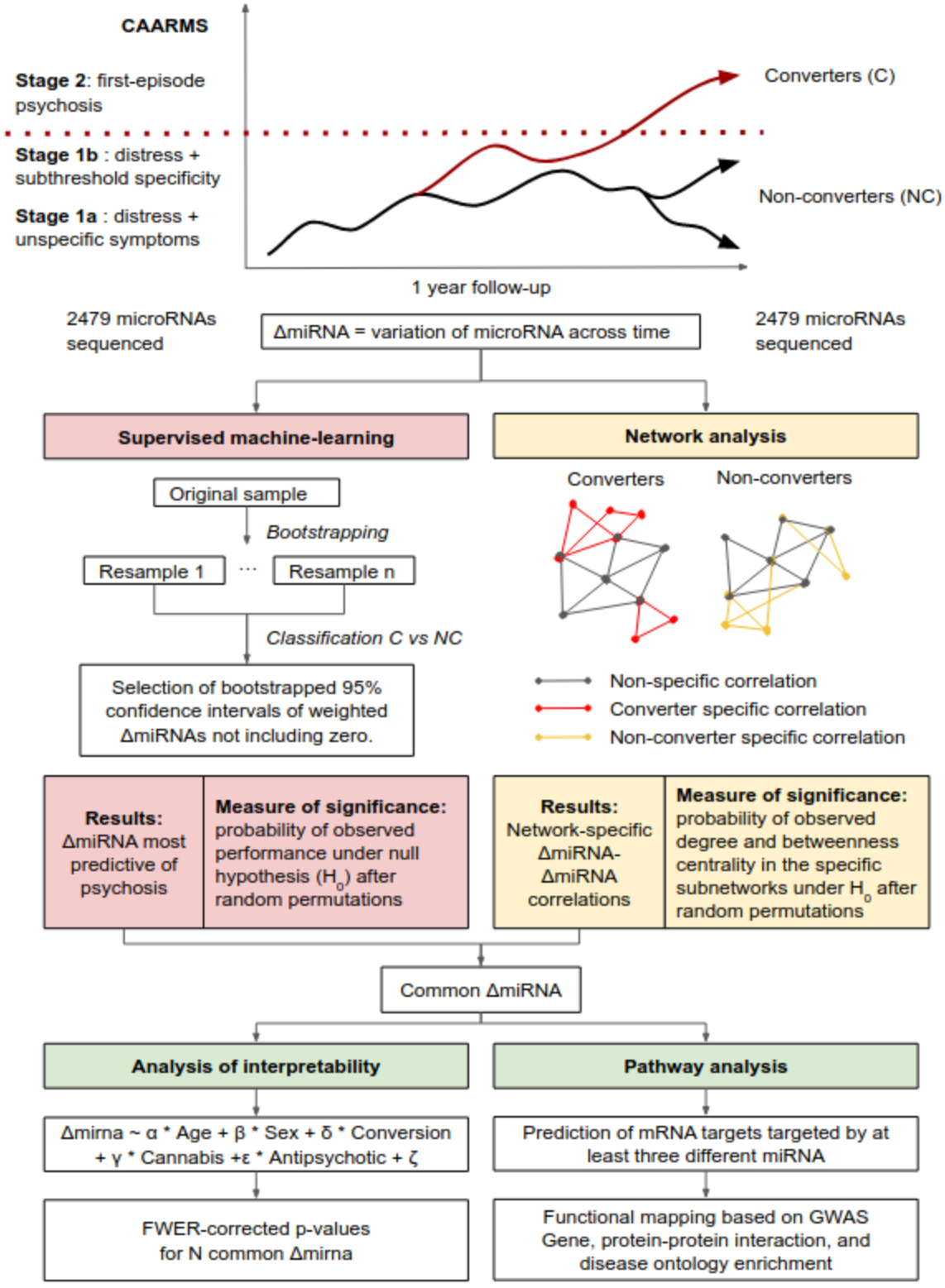
CAARMS
Stage 2: first-episode psychosis
Stage 1b : distress + subthreshold specificity
Stage 1a : distress + unspecific symptoms
Converters (C)
Non-converters (NC)
1 year follow-up
2479 microRNAs sequenced
ΔmiRNA = variation of microRNA across time
2479 microRNAs sequenced
Supervised machine-learning
Network analysis
Original sample
Bootstrapping
Resample 1
Resample n
Classification C vs NC
Selection of bootstrapped 95% confidence intervals of weighted ΔmiRNAs not including zero.
Converters
Non-converters
Non-specific correlation
Converter specific correlation
Non-converter specific correlation
Results: ΔmiRNA most predictive of psychosis
Measure of significance: probability of observed performance under null hypothesis (H_0) after random permutations
Results: Network-specific ΔmiRNA-ΔmiRNA correlations
Measure of significance: probability of observed degree and betweenness centrality in the specific subnetworks under H_0 after random permutations
Common ΔmiRNA
Analysis of interpretability
Pathway analysis
Δmirna ~ α * Age + β * Sex + δ * Conversion + γ * Cannabis +ε * Antipsychotic + ζ
Prediction of mRNA targets targeted by at least three different miRNA
FWER-corrected p-values for N common Δmirna
Functional mapping based on GWAS Gene, protein-protein interaction, and disease ontology enrichment

METHODS

Participants

Help-seeking and at-risk adolescents and young adults less than 30 years old were enrolled in a prospective cohort. All individuals were assessed with the CAARMS[28]. Psychotic conversion was characterized using the CAARMS-defined psychosis onset threshold. Individuals who reached the threshold during the one-year follow-up were considered converters and individuals who recovered or displayed persistent subthreshold symptoms were called non-converters. Demographic and clinical characteristics are described in **Table 1**. The study was approved by the institutional ethics committees (Comités de protection des personnes, Ile-de-France III and IV, Paris, France). Written informed consent was obtained from all participants or their legal representatives.

MicroRNA sequencing and preprocessing

Biological samples were obtained from the Biological Resource Center NSPN, GHU Paris Psychiatrie & Neurosciences, in charge of centralizing and managing biological data collection (BB-0033-00026). High-throughput sequencing was applied on the plasma of 81 samples at two time-points, baseline and follow-up. miRNAs were extracted with miRNeasy Serum/Plasma Advanced Kit (QIAGEN), then the standard workflow of the QIAseq® miRNA Library Kit (QIAGEN) was followed for library preparation, using unique molecular index assignment. Sequencing was performed on the Illumina NextSeq 500 platform at ICM of Hôpital de la Salpêtrière. Sequencing files were uploaded to QIAGEN GeneGlobe® Data Analysis Center to run QIAseq® miRNA Primary Quantification. Average total reads were 17.5 millions, 23.2% of total reads were UMI-assigned and 26.9% of these reads were aligned to 2479 miRNAs. Standard DESeq2 variance stabilizing transformation on R 3.6.3 was applied to obtain similar distributional properties (**Supplementary Figure 1**), increasing comparability across samples.[29] The variation of microRNA across time, Δmirna, was computed as the difference in transformed counts between follow-up and baseline, divided by the time between the two sampling events.

Table 1 - Demographic and clinical characteristics of the longitudinal cohort. PANSS: Positive And Negative Syndrome Scale. SOFAS: Social and Occupational Functioning Assessment Scale. MADRS: Montgomery–Åsberg Depression Rating Scale

	UHR longitudinal cohort		***T-test or X^2 for proportions***	
Measure	***Converters (35)*** *mean ± std*	***Non-Converters (46)*** *mean ± std*	***Test statistic***	***P-value***
Age at baseline	21.1 ± 3.4	22.6 ± 3.2	-1.95	**0.05**
Sex (F/M)	13 / 22	22 / 24	1.34	0.25
Duration of follow-up (years)	0.8 ± 0.5	1.2 ± 0.4	-3.67	**0.0004**
MADRS	22.2 ± 9.0	21.4 ± 10.2	0.35	0.72
PANSS total	70.0 ± 16.5	67.0 ± 16.7	0.77	0.44
positive	14.9 ± 5.0	12.4 ± 4.5	2.38	**0.02**
negative	15.5 ± 6.7	16.1 ± 7.4	-0.39	0.70
desorganisation	6.5 ± 3.1	5.6 ± 2.6	1.28	0.20
SOFAS	45.8 ± 11.2	46.7 ± 9.9	-0.35	0.73
Antipsychotics (%)	20 (7/35)	23.9 (11/46)	0.35	0.55
Chlorpromazine equivalent (mg)	25.9 ± 81.5	27.1 ± 57.5	-0.07	0.94
Cannabis last month (%)	37.1 (13/35)	15.2 (7/46)	9.18	**0.002**

Supervised learning algorithm

With the Scikit-learn python library,[30] we applied a stratified 5-fold nested cross-validation on an input matrix of subjects (81 rows) x Δmirna (2479 columns), in order to classify between converters and non-converters. The classifier was a logistic regression with: i) a norm L2 penalty, chosen because it outputs weights for each variable, allowing interpretation of each weighted Δmirna relative to the others, ii) a nested cross-validation with hyperparameter setting inside the training loop, using gridsearch (from C = $1e^{-6}$, for strong regularization in a high multi-dimensionality and multicollinearity problem, to no regularization with C = 1, with a discrete step of 0.1), and iii) a class weight set to “balanced” to account for the higher frequency of non-converters. Analysis steps are described in **Supplementary Figure 2**.

A robust non-parametric significance (p-value) for the observed AUC was computed through simulation-based random permutation analysis, whereby we simulated the null hypothesis by randomly permuting converter and non-converter statuses among subjects, and repeated the

algorithm 10 000 times. We then computed how many times the average AUC was higher or equal to the observed one. The reported p-value was calculated as the ratio of this number to the total number of tests done (10 000).

Non-parametric confidence intervals at 95 % (95%CI) for each Δmirna weight were computed by bootstrapping: estimates of the variance were obtained by averaging the predicted weights across 1000 bootstrap replications. Standard errors and 95%CI were obtained by calculating the standard deviations and the 2.5th and 97.5th percentiles of the bootstrapped distributions. The significance of the variance was derived from the 95%CI: the null hypothesis corresponding to a mean variance of zero was rejected when the 95%CI did not include zero.[31] This allowed to identify the Δmirna most contributing to the prediction.

Network analysis

Prior to graph analysis, all input Δmirna were adjusted for age and sex. To identify disease-specific interactions between Δmirna, we considered the matrix of correlations between all 2479 Δmirna in each group. We built two separate networks of correlations of longitudinal expression variation, and filtered only for strong correlations, above 0.7 in absolute value. A t-test was used to compare the distributions of betweenness and degree in the converters-specific subnetwork to the rest of the network. As a network metric, we measured the density of the converters-specific subnetwork. For betweenness and degree comparisons, as well as density measures, we tested the probability of obtaining the observed results under the null hypothesis of no Δmirna specificity by comparing them to randomly generated subnetworks[32], using permutations to compute non-parametric p-values as described in the previous section.

Pathway analysis

Pathway analysis was done on the intersection results of machine-learning and network analyses. miRDip v4.1 was used for prediction of mRNA targets of microRNAs.[33] Were selected only the “very high” confidence gene targets (the top 1% predicted by mirDIP) targeted by at least three different microRNAs to account for co-targeting mechanisms.[26] Two separate enrichment studies were done: i) functional mapping and association with human diseases based on genome-wide association studies was done with FUMA GWAS[34]; ii) gene, protein-protein interaction, and disease ontology enrichment were computed with Metascape[35].

Univariate statistical analysis.

Comparison of demographic and clinical data between groups were tested with a T-test for means or a Chi²-test for proportions. Spearman's ρ was used for correlation tests. In the differential expression analysis testing the interpretability of the 25 top Δmirna, we used the following linear model for each Δmirna: $\Delta mirna = intercept + \alpha * Age + \beta * Sex + \gamma * Conversion$. A second model also including cannabis use in the last month and antipsychotic medication as covariates was tested to account for their effects. Multiple testing was corrected with non-parametric permutation-based estimations of adjusted p-values obtained with the max-T procedure (resulting in FWER-corrected p-value), which is recommended for microarray experiments.[36,37] Volcano plot representation in python was done with bioinfokit.[38]

Results

Which subset among all Δmirna contributed most to predict psychosis ?

We used a supervised machine-learning strategy, leveraging all 2479 Δmirna for all 81 subjects, adjusted for age and sex, as input to a supervised learning algorithm, which we built to classify between converters and non-converters to psychosis. This allowed us to assess the relative weighted contribution of each Δmirna to the difference in outcome. The classifier showed a cross-validated performance with an area-under-the-curve (AUC) of 66 % and a balanced accuracy of 63 %. The average specificity is 0.74 and sensitivity is 0.51. The F-measure is 0.55. Repeated analysis after random permutation of status labels illustrated the fact that: i) the AUC's non-parametric p-value was significant (p = 0.009); and ii) there was no overfitting since the application of the same algorithm to randomly labeled subjects led to an average classification, under the null hypothesis, with an AUC of 50 %, i.e. no better than chance (**Supplementary Figure 3**). We identified 207 Δmirna that significantly participated in the classification between converters and non-converters, with predicted weights confidently different from zero (at 95 %), either positive or negative (**Supplementary Figure 4**).

Which Δmirna were specific to the outcome (conversion or non conversion) ?

To further identify interacting microRNAs with discriminative power across time between converters and non-converters, we considered the matrix of correlations between all 2479 Δmirna in each group, adjusted beforehand for age and sex. We found 243 Δmirna to be specific to the converters' network, and 33 Δmirna specific to the non-converters'. Individual and network metrics of the converters-specific Δmirna subnetwork were compared to the rest of the converters-network (including Δmirna not specific to conversion). For each node in the graph, corresponding to a Δmirna, we computed betweenness centrality and degree centrality. The former measures to what extent a node is a bottleneck in the network (i.e. the number of shortest paths between all pairs of nodes that go through this node), and the latter measures to what extent a node is a hub (i.e the number of edges connected to this node).[39,40] Inside the converters' network, betweenness centrality was four times higher in the conversion-specific subnetwork of Δmirna (mean: $1.6e^{-3}$) compared to the rest of the network (mean: $0.4e^{-3}$). This was significant after random permutations to simulate the null hypothesis of no specificity of microRNAs (p=0.002). Conversely, degree centrality was four times lower in the conversion-specific subnetwork of Δmirna (mean: 305) compared to the rest of the network (mean: 1307). This was significant after random permutations to simulate the null hypothesis of no specificity of microRNAs (p=0.001) (**Figure 2**). Likewise, the density in the conversion-specific subnetwork was very low (0.03) compared to what could be expected by randomly selecting 243 Δmirna in the network (0.5 on average), with a non-parametric p-value of 0.001.

Pathway analysis of top microRNAs resulting for both strategies

By intersecting the 207 microRNAs from the machine learning analysis, whose absolute variation across time predicted the emergence of psychosis, with the 276 microRNAs that had correlations of variation specific to one network, we found 25 microRNAs whose changes in expression across time could have network-level significance and be therefore more relevant from a pathophysiological perspective. Looking at only highly confident mRNA predicted targets of these microRNAs, 438 genes were identified. The top GWAS enrichment was general cognitive ability (adjusted $p < 10^{-4}$), but also genes pleiotropically associated with cognitive ability, educational attainment and schizophrenia (adjusted $p < 10^{-2}$) (**Figure 3a**). Moreover, the top gene ontology enrichments included transcriptional regulation by the methyl-CpG binding protein 2 (MECP2) and brain development ($p < 10^{-8}$), as well as synaptic signaling ($p < 10^{-6}$)

(**Figure 3b**). The top affected protein-protein interactions included oxidative stress-induced senescence ($p < 10^{-16}$), membrane trafficking processes ($p < 10^{-12}$), signal transduction mechanisms ($p < 10^{-12}$), as well as neuron apoptotic processes ($p < 10^{-5}$) (**Figure 3c**). Gene-disease association analysis showed that the top significantly enriched diseases included neurodevelopmental disorders and developmental delay ($p < 10^{-10}$) (**Figure 3d**).

FIgure 2 - Relationship between degree and betweenness centrality in the converters' network. 3a) Converter-specific microRNA variations have higher betweenness and lower degree centrality compared to non-specific microRNAs. 3b) Illustration of bottleneck nodes with high betweenness/low degree (red) and hub nodes with high degree (blue circle). For betweenness and degree comparisons, as well as density measures, we tested the probability of obtaining the observed results under the null hypothesis of no Δmirna specificity by comparing them to randomly generated subnetworks, using permutations to compute non-parametric p-values.

2a)

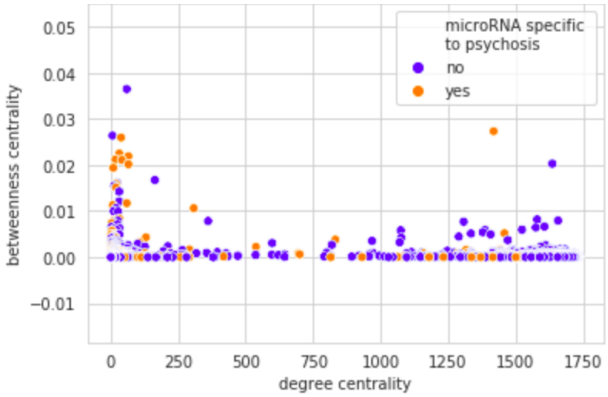

2b)

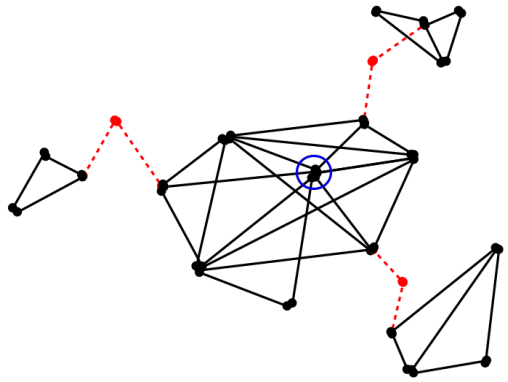

Figure 3 - Enrichment analysis

3a)

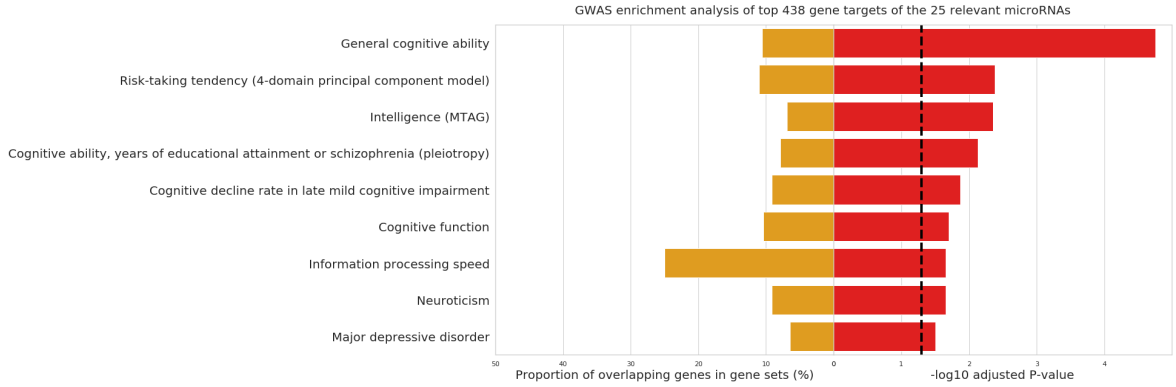

3b)

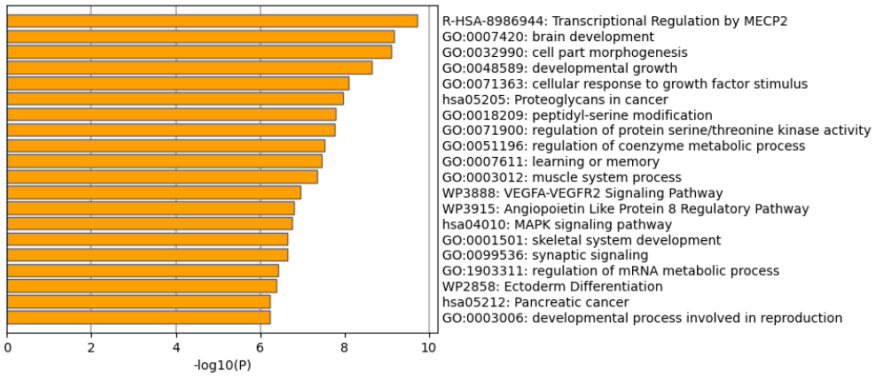

3c)

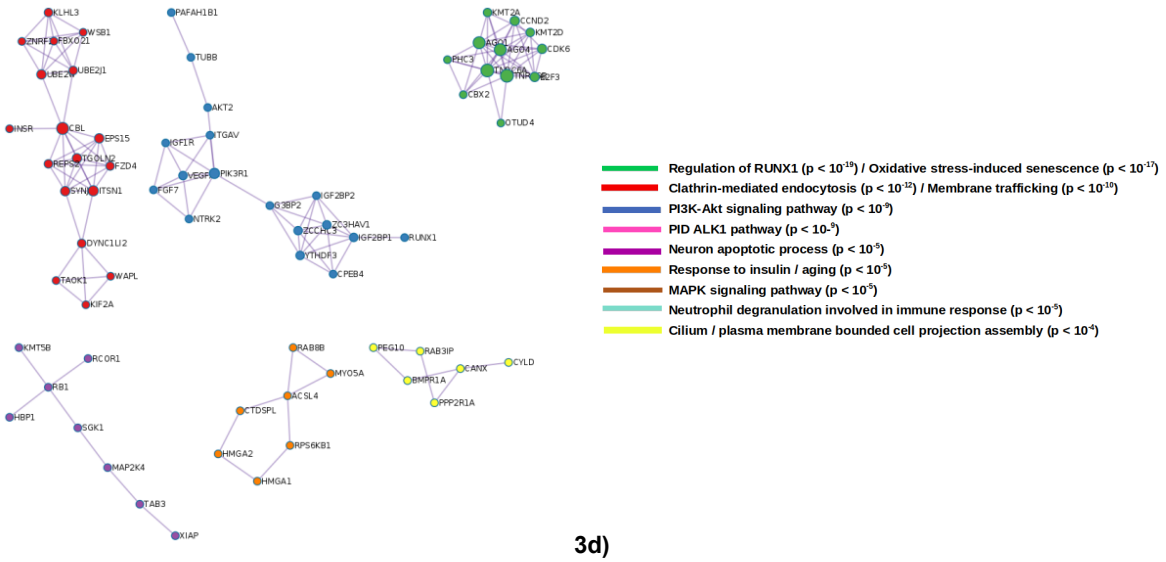

3d)

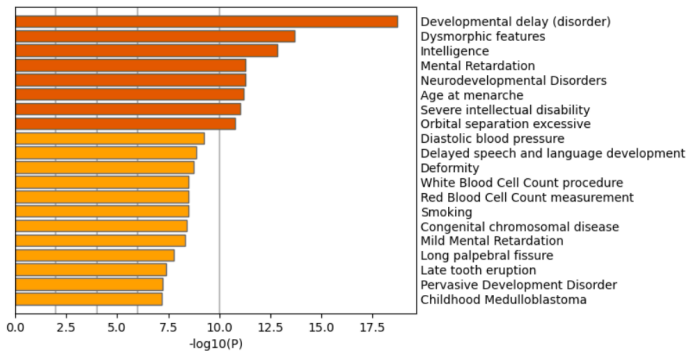

Testing the interpretability of the resulting Δmirna in relation to conversion to psychosis

Although significant positive or negative weights of Δmirna in the classifier algorithm may reflect an important contribution to the outcome of interest (here, classification of the disease trajectory), they could also represent suppression of noisy data specific to this cohort that would

be pathophysiologically irrelevant. Parameters of multivariate classifiers, defined as *backward models* where the variable of interest (i.e. outcome) is expressed as a function of the data (i.e. Δmirna), are therefore not directly interpretable. Conversely, *forward models* where the data is expressed as a function of variables of interest provide interpretable parameters.[27] For this reason, and to identify the microRNAs with the highest confidence, we used univariate analysis to express the resulting 25 Δmirna of interest as functions of age, sex, clinical outcome. After correction for multiple testing, two microRNAs showed longitudinal variations significantly associated with outcome: miR-150-5p and miR-3191-5p (**Figure 4**).

FIgure 4 - 4a) Longitudinal variation across time of miR-150-5p and miR-3191-5p expression in converters and non-converters. Counts represent values after variance stabilizing transformation of raw counts with DESeq2. 4b) Volcano plot representing the level and direction of microRNA variation across time associated with conversion to psychosis, and corrected for the FWER, for the 25 microRNAs of interest in all subjects.

4a)

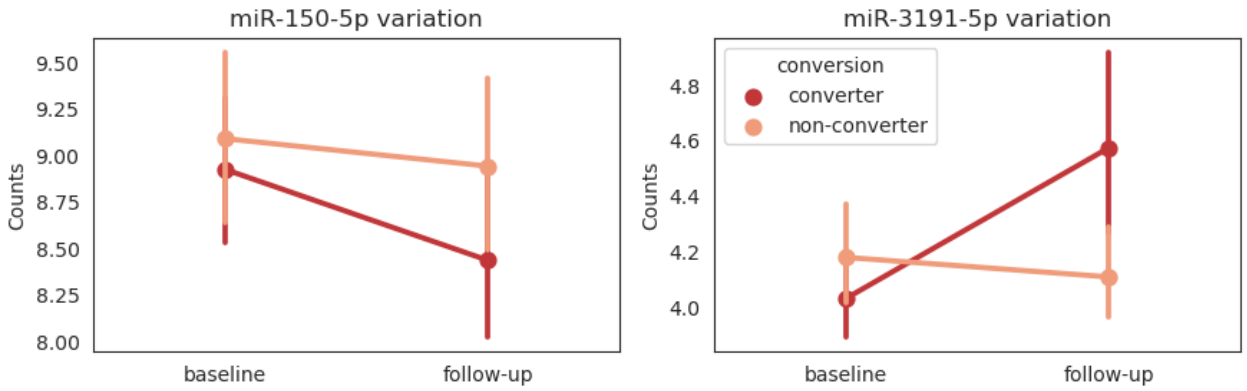

4b)

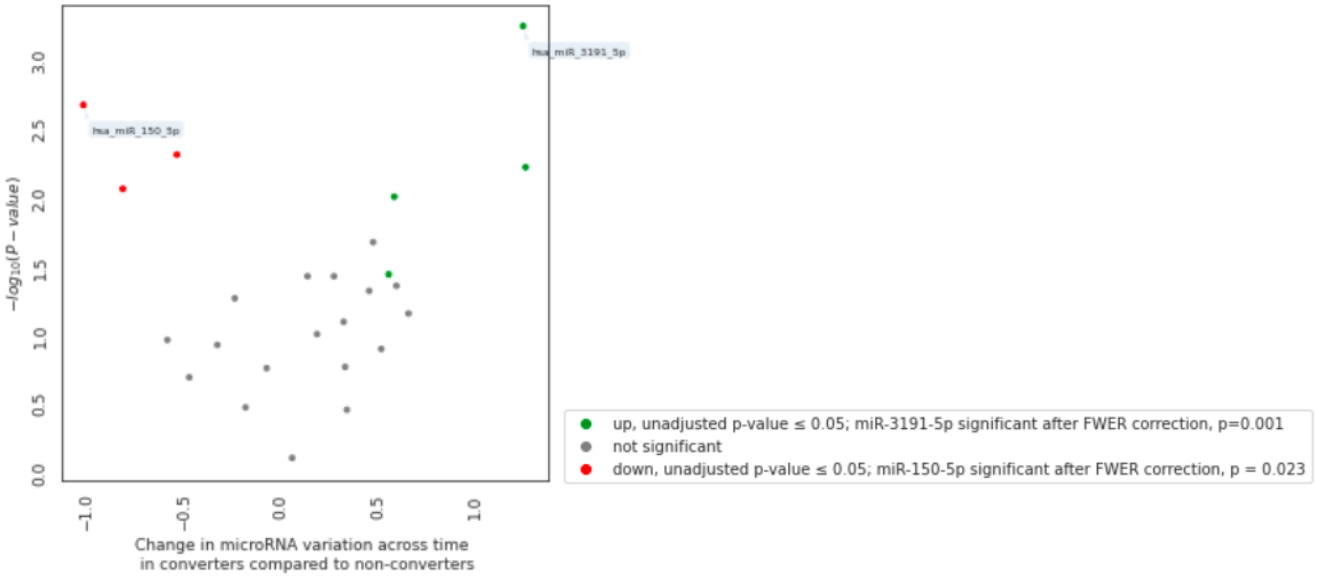

There was a significant longitudinal decrease in miR-150-5p expression in converters compared to non-converters (β = -1.02, adjusted-p = 0.023, 95%CI = [-1.67, -0.37]). Age and sex did not significantly explain this effect (p = 0.25 and p = 0.14, respectively). This decrease remained significant after adding cannabis intake in the last month and antipsychotic medication as a covariates (β = -1.00, p = 0.004, 95%CI = [-1.68, -0.33]). Neither cannabis use nor medication significantly explained the decrease (p = 0.87 and p = 0.51, respectively). There was a significant longitudinal increase in miR-3191-5p expression in converters compared to non-converters (β = 1.39, p = 0.0002, 95%CI = [0.69, 2.08]). Age at baseline also significantly explained this effect (β = 0.14, p = 0.009, 95%CI = [0.03, 0.24]). Cannabis use did not significantly explain this increase (p = 0.09), but medication intake significantly explained it, albeit with a small effect (β = 0.01, p = 0.038, 95%CI = [0.0003, 0.01]).

DISCUSSION

In this first longitudinal study of microRNA variation during conversion to psychosis, in an UHR population with high-throughput microRNA sequencing available at two time-points, we identified a dynamic epigenetic signature of the emergence of psychosis that is pathophysiologically relevant.

First, we accounted for microRNA-microRNA cooperation and co-regulatory mechanisms[25,26] by using a machine-learning strategy, leveraging all 2479 longitudinal microRNA variations for all 81 subjects as input to a supervised learning algorithm, to classify between converters and non-converters to psychosis. This allowed us to assess the relative weighted contribution of each longitudinal microRNA variation to the difference in outcome. Whereas our longitudinal design is not comparable with previous cross-sectional results, two of our 207 microRNAs overlapped with the 15 microRNAs reported as “the most recurrent and representative differentially expressed microRNAs” in case-control studies[7]. This overlap contained miR-30e and miR-137, the latter being a microRNA strongly involved in neural pathways disrupted in schizophrenia[8], consistently differentially expressed in this disease[7], associated with schizophrenia in genome-wide association studies (GWAS)[41], and known to regulate schizophrenia-risk genes[42].

Secondly, to further account for the complex interplay between many microRNA longitudinal variations, we considered the correlation network of microRNA variations in converters and non-converters separately. Using a strong threshold of 0.7 for the correlations, above the 0.3-0.4

commonly observed in biology[43], we identified the most robust nodes specific to each network. Differential network analysis highlighted 276 microRNAs specific to one network. Among these, 243 were specific to the converters' network. Compared to the rest of the converters' network, longitudinal microRNA variations in this specific subnetwork showed significantly higher betweenness centrality, lower degree centrality and lower density. This might suggest that although the conversion-specific microRNA variations are topographically sparse and not necessarily connected with each other, they could play important roles as mediators in the whole correlation network. Thus, betweenness centrality was found to be more important than degree centrality for regulatory network integrity in protein-protein interactions, where high betweenness/low degree members appeared to be involved in regulation and signal transduction[44].

Thirdly, by intersecting the 207 microRNAs whose longitudinal variation predicted psychosis with the 276 microRNAs that had correlations of variation specific to one network, we obtained 25 microRNAs whose longitudinal changes could have network-level significance and therefore be more relevant from a pathophysiological perspective. Their mRNA targets were enriched in cognition and schizophrenia GWAS-associated genes, and gene ontology enrichment highlighted neurodevelopmental processes and MECP2 regulation. MECP2 controls regulation of gene expression and is involved in neuronal and synaptic development. Its activity could be modulated by neuronal activity, suggesting a role in plasticity[45]. Moreover, rare mutations in the *MECP2* gene have been found in neurodevelopmental disorders, especially Rett's syndrome, but also in schizophrenia[46], and increased MECP2 promoter binding in GABAergic neurons of the frontal cortex and hippocampus was described in a mice model of prenatal stress leading to psychotic-like phenotypes[47]. The enriched oxidative stress-related pathways have also been identified as dysregulated in psychosis, and described in UHR during conversion to psychosis by our previous methylome and transcriptome analyses[9,10].

Finally, knowing that machine-learning strategies are *backward models* that do not provide straightforward pathophysiologically interpretable models, but solutions that may also depend on noise correction[27], we further tested the interpretability of the resulting 25 microRNAs by reversing the analysis for the top 25 microRNAs into classical *forward models* where univariate analysis allowed to test the dependency of longitudinal microRNA variation on clinically relevant variables. We identified mir-150-5p's decrease and miR-3191-5p's increase to be significantly

associated with the emergence of psychosis, independently of age, sex, cannabis intake in the last month, and antipsychotic use.

miR-150 is a precursor microRNA that is processed in two mature forms (miR-150-5p and miR-150-3p). This precursor was reported to be downregulated in individuals with schizophrenia, both in peripheral blood mononuclear cells[48] and in neurons from the superior temporal gyrus[49]. miR-150-5p is also known to be significantly downregulated in individuals with 22q11 deletion syndrome, compared to healthy controls[50]. This syndrome is the most frequent genetic cause of schizophrenia with around 40% of the 22q11 carriers who will develop a psychotic disorder[51]. Finally, miR-150-5p was recently found to be among six microRNAs consistently downregulated in a cohort of children with autism spectrum disorder compared to healthy controls, in clinically unaffected parents at genetic risk, and in a corresponding mouse model[52]. Because autism and schizophrenia are on a neurodevelopmental continuum, miR-150-5p downregulation could be one of their shared genetic and epigenetic pathways[53]. Since its induced increase rescued cognitive dysfunction in a rat model[54], miR-150 could also constitute a target for treatment. Information regarding miR-3191-5p in relation to psychosis is lacking in the literature. Nevertheless, it was reported to be downregulated in a cross-sectional study of the microRNA system in schizophrenia,[55] and an animal model found that it inhibited the expression of *CACNA1A*, a gene whose function is involved in cerebellar development.[56]

There are several considerations that should be taken into account. Crossing two data-driven strategies, we reduced the risk of methodological biases associated with any single method, while including all sequenced microRNAs in the analysis. Using a longitudinal design allowed to account for intra-individual variations, increasing the power to detect significant changes. Regarding prediction, the performance was robust and not overfitting on random noise, but it was not sufficiently high for clinical implementation. This was to be expected as microRNAs represent only a small fraction of the many biological levels involved in the pathophysiology of psychosis. Thus, our performance falls in the average of performances reported with structural neuroimaging-based predictions of first-episode psychosis, which range between chance level and 85%[57]. Because of a lack of other available cohorts with longitudinal microRNA sampling, cross-validation was used to test the prediction. However, testing in an independent cohort would be required for definitive validation. As it is, we suggest this method be combined with other data-driven or selection-based procedures only as a strategy to increase confidence in microRNA analysis. Regarding network analysis, the main limitation is the biological meaning of

a correlation between two microRNAs across time, which remains to be further explored[43]. Likewise, betweenness centrality is a more relevant concept in directed (regulatory) networks, than in undirected (interaction) ones. We postulated this was the case with microRNAs, but it remains to be confirmed. Building correlation-based networks was necessary to be able to compare groups. Moreover, we chose to compare networks built on longitudinal microRNA variation, rather than comparing network preservation between baseline and follow-up in each group. Because correlations are adimensional measures, a correlation between two baseline microRNA expressions will not change at follow-up if one of them decreases its expression. Therefore, our longitudinal design allowed us to highlight differences that would otherwise have gone unnoticed. Regarding enrichment analyses, their interpretation is limited by what it means to be a mRNA target of a microRNA. Thus, while microRNAs mainly downregulate translation, the reverse can also be true.[58] The question of the relevance of peripheral blood sampling for brain physiology is another limit, but peripheral sampling was necessary for clinical biomarker research. In the gene-environment paradigm, the same environmental stressors that affect the brain may be expected to have similar effects in other tissues, and the regulation of miRNA expression is strongly under genetic influence, which is identical between brain and blood cells. Finally, our results do not infer causality but provide a longitudinal correlational signature of disease.

In conclusion, this is the first study identifying twenty-five microRNAs whose longitudinal variations could be a dynamic signature of the emergence of psychosis. The genes targeted by these microRNAs are overrepresented in cognitive measures and schizophrenia GWAS findings, in genes regulated by MECP2 and in pathways related to brain development, synaptic signaling and oxidative stress. Two microRNAs, miR-150-5p and miR-3191-5p, have emerged as the most promising for better insight into the longitudinal epigenetic changes associated with psychosis progression.

Acknowledgements

We thank the patients for their participation and their trust. We thank the ICAAR-START Study Group (Julie Bourgin, Claire Daban Huard, Célia Jantac Mam-Lam-Fook, Gilles Martinez, Marion Plaze, Fabrice Rivollier, Mathilde Kazes). We thank Yveline Lepaicheux and Itri El Karchani for the sampling. We thank Yannick Marie for the microRNA sequencing, along with

Thomas Gareau and Justine Guegan, for their statistical advice (ICM-Paris Brain Institute). We benefited from equipment from the iGenSeq core facility, at ICM.

Funding

This work was funded by ANR Epi-Young (ANR-17-CE37-0003-01) and Fédération pour la Recherche sur le Cerveau. It has been supported by the French government's "Investissements d'Avenir" programme (ANR-18-RHUS-0014 PsyCARE), French Ministry grants PHRC AOM07-118 (ICAAR) and PHRC 13-0681 (START). Boris Chaumette receives a grant from Fondation Bettencourt Schueller (CCA INSERM Bettencourt). Anton Iftimovici received a fellowship from Fondation pour la Recherche Médicale (FRM).

Conflict of Interest

The Authors have declared that there are no conflicts of interest in relation to the subject of this study.

Availability of data

The data supporting this study and the python script containing each analysis step are available upon reasonable request.

References

1. Solmi M, Radua J, Olivola M, et al. Age at onset of mental disorders worldwide: large-scale meta-analysis of 192 epidemiological studies. *Mol Psychiatry*. Published online June 2, 2021. doi:10.1038/s41380-021-01161-7
2. Fusar-Poli P, Salazar de Pablo G, Correll CU, et al. Prevention of Psychosis: Advances in Detection, Prognosis, and Intervention. *JAMA Psychiatry*. 2020;77(7):755. doi:10.1001/jamapsychiatry.2019.4779
3. Salazar de Pablo G, Radua J, Pereira J, et al. Probability of Transition to Psychosis in Individuals at Clinical High Risk: An Updated Meta-analysis. *JAMA Psychiatry*. Published online July 14, 2021. doi:10.1001/jamapsychiatry.2021.0830
4. Howes OD, Murray RM. Schizophrenia: an integrated sociodevelopmental-cognitive model. *The Lancet*. 2014;383(9929):1677-1687. doi:10.1016/S0140-6736(13)62036-X
5. McCutcheon RA, Reis Marques T, Howes OD. Schizophrenia—An Overview. *JAMA Psychiatry*. Published online October 30, 2019:1. doi:10.1001/jamapsychiatry.2019.3360
6. Birnbaum R, Weinberger DR. Genetic insights into the neurodevelopmental origins of schizophrenia. *Nat Rev Neurosci*. 2017;18(12):727-740. doi:10.1038/nrn.2017.125

7. Smigielski L, Jagannath V, Rössler W, Walitza S, Grünblatt E. Epigenetic mechanisms in schizophrenia and other psychotic disorders: a systematic review of empirical human findings. *Mol Psychiatry*. Published online January 6, 2020. doi:10.1038/s41380-019-0601-3
8. Richetto J, Meyer U. Epigenetic Modifications in Schizophrenia and Related Disorders: Molecular Scars of Environmental Exposures and Source of Phenotypic Variability. *Biol Psychiatry*. Published online March 2020:S0006322320313275. doi:10.1016/j.biopsych.2020.03.008
9. Kebir O, Chaumette B, Rivollier F, et al. Methylomic changes during conversion to psychosis. *Mol Psychiatry*. 2017;22(4):512-518. doi:10.1038/mp.2016.53
10. Chaumette B, Kebir O, Pouch J, et al. Longitudinal Analyses of Blood Transcriptome During Conversion to Psychosis. *Schizophr Bull*. 2019;45(1):247-255. doi:10.1093/schbul/sby009
11. Jeffries CD, Perkins DO, Chandler SD, et al. Insights into psychosis risk from leukocyte microRNA expression. *Transl Psychiatry*. 2016;6(12):e981-e981. doi:10.1038/tp.2016.148
12. Krützfeldt J, Poy MN, Stoffel M. Strategies to determine the biological function of microRNAs. *Nat Genet*. 2006;38(S6):S14-S19. doi:10.1038/ng1799
13. Gibbons A, Udawela M, Dean B. Non-Coding RNA as Novel Players in the Pathophysiology of Schizophrenia. *Non-Coding RNA*. 2018;4(2):11. doi:10.3390/ncrna4020011
14. Hauberg ME, Roussos P, Grove J, Børglum AD, Mattheisen M, for the Schizophrenia Working Group of the Psychiatric Genomics Consortium. Analyzing the Role of MicroRNAs in Schizophrenia in the Context of Common Genetic Risk Variants. *JAMA Psychiatry*. 2016;73(4):369. doi:10.1001/jamapsychiatry.2015.3018
15. Zhang HC, Du Y, Chen L, Yuan ZQ, Cheng Y. MicroRNA schizophrenia: Etiology, biomarkers and therapeutic targets. *Neurosci Biobehav Rev*. 2023;146:105064. doi:10.1016/j.neubiorev.2023.105064
16. Olde Loohuis NFM, Ba W, Stoerchel PH, et al. MicroRNA-137 Controls AMPA-Receptor-Mediated Transmission and mGluR-Dependent LTD. *Cell Rep*. 2015;11(12):1876-1884. doi:10.1016/j.celrep.2015.05.040
17. Chun S, Du F, Westmoreland JJ, et al. Thalamic miR-338-3p mediates auditory thalamocortical disruption and its late onset in models of 22q11.2 microdeletion. *Nat Med*. 2017;23(1):39-48. doi:10.1038/nm.4240
18. Bahi A, Dreyer JL. Lentiviral-mediated let-7d microRNA overexpression induced anxiolytic- and anti-depressant-like behaviors and impaired dopamine D3 receptor expression. *Eur Neuropsychopharmacol*. 2018;28(12):1394-1404. doi:10.1016/j.euroneuro.2018.09.004
19. Ma K, Zhang H, Wang S, et al. The molecular mechanism underlying GABAergic dysfunction in nucleus accumbens of depression‐like behaviours in mice. *J Cell Mol Med*. 2019;23(10):7021-7028. doi:10.1111/jcmm.14596
20. Lai CY, Lee SY, Scarr E, et al. Aberrant expression of microRNAs as biomarker for schizophrenia: from acute state to partial remission and from peripheral blood to cortical tissue. *Transl Psychiatry*. 2016;6(1):e717-e717. doi:10.1038/tp.2015.213
21. Wei H, Yuan Y, Liu S, et al. Detection of Circulating miRNA Levels in Schizophrenia. *Am J Psychiatry*. 2015;172(11):1141-1147. doi:10.1176/appi.ajp.2015.14030273
22. Yu H chuan, Wu J, Zhang H xing, et al. Alterations of miR-132 are novel diagnostic biomarkers in peripheral blood of schizophrenia patients. *Prog Neuropsychopharmacol Biol Psychiatry*. 2015;63:23-29. doi:10.1016/j.pnpbp.2015.05.007
23. Sun X yang, Zhang J, Niu W, et al. A preliminary analysis of microRNA as potential clinical biomarker for schizophrenia. *Am J Med Genet B Neuropsychiatr Genet*. 2015;168(3):170-178. doi:10.1002/ajmg.b.32292
24. Nelson B, McGorry PD, Wichers M, Wigman JTW, Hartmann JA. Moving From Static to

Dynamic Models of the Onset of Mental Disorder: A Review. *JAMA Psychiatry*. 2017;74(5):528. doi:10.1001/jamapsychiatry.2017.0001
25. Obermayer B, Levine E. Exploring the miRNA Regulatory Network Using Evolutionary Correlations. *PLOS Comput Biol*. 2014;10(10):13.
26. Cherone JM, Jorgji V, Burge CB. Cotargeting among microRNAs in the brain. *Genome Res*. 2019;29(11):1791-1804. doi:10.1101/gr.249201.119
27. Haufe S, Meinecke F, Görgen K, et al. On the interpretation of weight vectors of linear models in multivariate neuroimaging. *NeuroImage*. 2014;87:96-110. doi:10.1016/j.neuroimage.2013.10.067
28. Yung AR, Yuen HP, Mcgorry PD, et al. Mapping the Onset of Psychosis: The Comprehensive Assessment of At-Risk Mental States. *Aust N Z J Psychiatry*. Published online 2005:39:964-971.
29. Anders S, Huber W. Differential expression analysis for sequence count data. Published online 2010:12.
30. Pedregosa F, Varoquaux G, Gramfort A, et al. Scikit-learn: Machine Learning in Python. *ArXiv12010490 Cs*. Published online June 5, 2018. Accessed November 23, 2019. http://arxiv.org/abs/1201.0490
31. B. Efron and R. Tibshirani. Bootstrap Methods for Standard Errors, Confidence Intervals, and Other Measures of Statistical Accuracy. *Stat Sci*. Published online 1986:1:54-75.
32. Halder AK, Denkiewicz M, Sengupta K, Basu S, Plewczynski D. Aggregated network centrality shows non-random structure of genomic and proteomic networks. *Methods*. 2020;181-182:5-14. doi:10.1016/j.ymeth.2019.11.006
33. Tokar T, Pastrello C, Rossos AEM, et al. mirDIP 4.1—integrative database of human microRNA target predictions. *Nucleic Acids Res*. 2018;46(D1):D360-D370. doi:10.1093/nar/gkx1144
34. Watanabe K, Taskesen E, van Bochoven A, Posthuma D. Functional mapping and annotation of genetic associations with FUMA. *Nat Commun*. 2017;8(1):1826. doi:10.1038/s41467-017-01261-5
35. Zhou Y, Zhou B, Pache L, et al. Metascape provides a biologist-oriented resource for the analysis of systems-level datasets. *Nat Commun*. 2019;10(1):1523. doi:10.1038/s41467-019-09234-6
36. Dudoit S, Shaffer JP, Block JC. Multiple Hypothesis Testing in Microarray Experiments. *Stat Sci*. 2003;18(1):71-103. doi:10.1214/ss/1056397487
37. Bourgon R, Gentleman R, Huber W. Independent filtering increases detection power for high-throughput experiments. *Proc Natl Acad Sci*. 2010;107(21):9546-9551. doi:10.1073/pnas.0914005107
38. Renesh Bedre. reneshbedre/bioinfokit: Bioinformatics data analysis and visualization toolkit. Published online January 6, 2021. doi:10.5281/zenodo.4422035
39. Hu JX, Thomas CE, Brunak S. Network biology concepts in complex disease comorbidities. *Nat Rev Genet*. 2016;17(10):615-629. doi:10.1038/nrg.2016.87
40. Barabási AL, Oltvai ZN. Network biology: understanding the cell's functional organization. *Nat Rev Genet*. 2004;5(2):101-113. doi:10.1038/nrg1272
41. The Schizophrenia Psychiatric Genome-Wide Association Study (GWAS) Consortium. Genome-wide association study identifies five new schizophrenia loci. *Nat Genet*. 2011;43(10):969-976. doi:10.1038/ng.940
42. Schizophrenia Working Group of the Psychiatric Genomics Consortium. Biological insights from 108 schizophrenia-associated genetic loci. *Nature*. 2014;511(7510):421-427. doi:10.1038/nature13595

43. Dragomir M, Mafra A, Dias S, Vasilescu C, Calin G. Using microRNA Networks to Understand Cancer. *Int J Mol Sci*. 2018;19(7):1871. doi:10.3390/ijms19071871
44. Haiyuan Yu , Philip M. Kim , Emmett Sprecher, Valery Trifonov, Mark Gerstein. The Importance of Bottlenecks in Protein Networks: Correlation with Gene Essentiality and Expression Dynamics. Published online 2007.
45. Tropea D, Mortimer N, Bellini S, et al. Expression of nuclear Methyl-CpG binding protein 2 (Mecp2) is dependent on neuronal stimulation and application of Insulin-like growth factor 1. *Neurosci Lett*. 2016;621:111-116. doi:10.1016/j.neulet.2016.04.024
46. Chen CH, Cheng MC, Huang A, Hu TM, Ping LY, Chang YS. Detection of Rare Methyl-CpG Binding Protein 2 Gene Missense Mutations in Patients With Schizophrenia. *Front Genet*. 2020;11:476. doi:10.3389/fgene.2020.00476
47. Matrisciano F, Tueting P, Dalal I, et al. Epigenetic modifications of GABAergic interneurons are associated with the schizophrenia-like phenotype induced by prenatal stress in mice. *Neuropharmacology*. 2013;68:184-194. doi:10.1016/j.neuropharm.2012.04.013
48. Gardiner E, Beveridge NJ, Wu JQ, et al. Imprinted DLK1-DIO3 region of 14q32 defines a schizophrenia-associated miRNA signature in peripheral blood mononuclear cells. *Mol Psychiatry*. 2012;17(8):827-840. doi:10.1038/mp.2011.78
49. Pietersen CY, Mauney SA, Kim SS, et al. Molecular Profiles of Parvalbumin-Immunoreactive Neurons in the Superior Temporal Cortex in Schizophrenia. *J Neurogenet*. 2014;28(1-2):70-85. doi:10.3109/01677063.2013.878339
50. Sellier C, Hwang VJ, Dandekar R, et al. Decreased DGCR8 Expression and miRNA Dysregulation in Individuals with 22q11.2 Deletion Syndrome. Cai T, ed. *PLoS ONE*. 2014;9(8):e103884. doi:10.1371/journal.pone.0103884
51. Karayiorgou M, Simon TJ, Gogos JA. 22q11.2 microdeletions: linking DNA structural variation to brain dysfunction and schizophrenia. *Nat Rev Neurosci*. 2010;11(6):402-416. doi:10.1038/nrn2841
52. Ozkul Y, Taheri S, Bayram KK, et al. A heritable profile of six miRNAs in autistic patients and mouse models. *Sci Rep*. 2020;10(1):9011. doi:10.1038/s41598-020-65847-8
53. Cattane N, Richetto J, Cattaneo A. Prenatal exposure to environmental insults and enhanced risk of developing Schizophrenia and Autism Spectrum Disorder: focus on biological pathways and epigenetic mechanisms. *Neurosci Biobehav Rev*. Published online July 2018:S0149763417309727. doi:10.1016/j.neubiorev.2018.07.001
54. Cui H, Xu Z, Qu C. Tetramethylpyrazine ameliorates isoflurane-induced cognitive dysfunction by inhibiting neuroinflammation via miR-150 in rats. *Exp Ther Med*. Published online 2020:10.
55. Zhang F, Xu Y, Shugart YY, et al. Converging Evidence Implicates the Abnormal MicroRNA System in Schizophrenia. *Schizophr Bull*. 2015;41(3):728-735. doi:10.1093/schbul/sbu148
56. Miyazaki Y, Du X, Muramatsu S ichi, Gomez CM. An miRNA-mediated therapy for SCA6 blocks IRES-driven translation of the *CACNA1A* second cistron. *Sci Transl Med*. 2016;8(347). doi:10.1126/scitranslmed.aaf5660
57. Vieira S, Gong Q yong, Pinaya WHL, et al. Using Machine Learning and Structural Neuroimaging to Detect First Episode Psychosis: Reconsidering the Evidence. *Schizophr Bull*. 2020;46(1):17-26. doi:10.1093/schbul/sby189
58. Vasudevan S, Tong Y, Steitz JA. Switching from Repression to Activation: MicroRNAs Can Up-Regulate Translation. *Science*. 2007;318(5858):1931-1934. doi:10.1126/science.1149460

SUPPLEMENTARY DATA

Supplementary Figure 1 - Pre and post-transformation plots. Pre- and post-distribution of mean and standard deviation of data: the transformation allows to correct for the lack of homoscedasticity that is intrinsically associated with RNA sequencing (because the more a couple of microRNAs are read in a sample, the less the other microRNAs are, leading to higher variances of reads in that specific sample); after DESeq2 variance stabilizing transformation, we see that the standard deviation is no longer correlated with the mean.

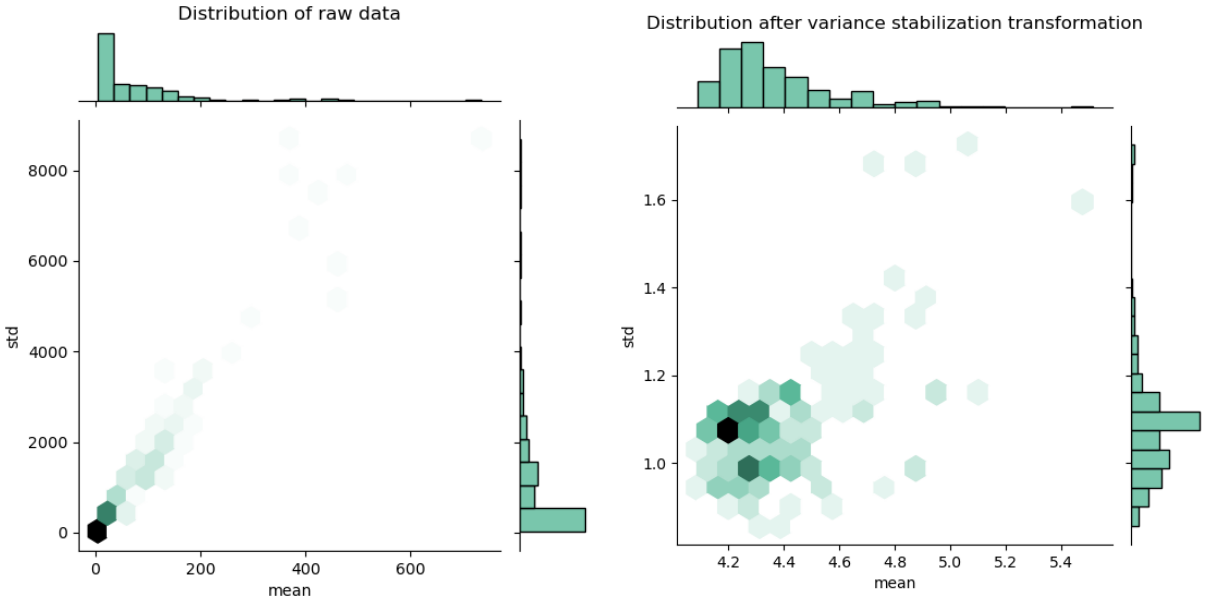

Supplementary Figure 2 - Supervised learning algorithm: stratified 5-fold cross-validation with residualization inside the training loops. Δmirna is a matrix of miRNA variations across time (as columns) for each subject (rows). The prediction model M is a logistic regression with L2 (ridge) penalty, using a nested cross-validation to set hyperparameter C, and a balanced class weight. In the training fold of each loop: i) residualizer function R regresses Δmirna of the training set to adjust for age and sex, in order to keep only the conversion-related variance and the noise for training ($R(\Delta mirna_{train})$); ii) a nested-cross-validation selects the best hyperparameter C; iii) a model M is fitted on the age- and sex-corrected training set. Then, in the testing fold of each loop: i) residualizer function R predicts the age- and sex-corrected testing set ($R(\Delta mirna_{test})$); importantly, the conversion information from the testing set is not used in the regression; ii) model M uses this corrected testing set to predict the conversion status. This process is repeated 5 times, giving 5 AUC and balanced accuracies, which are averaged for overall performance.

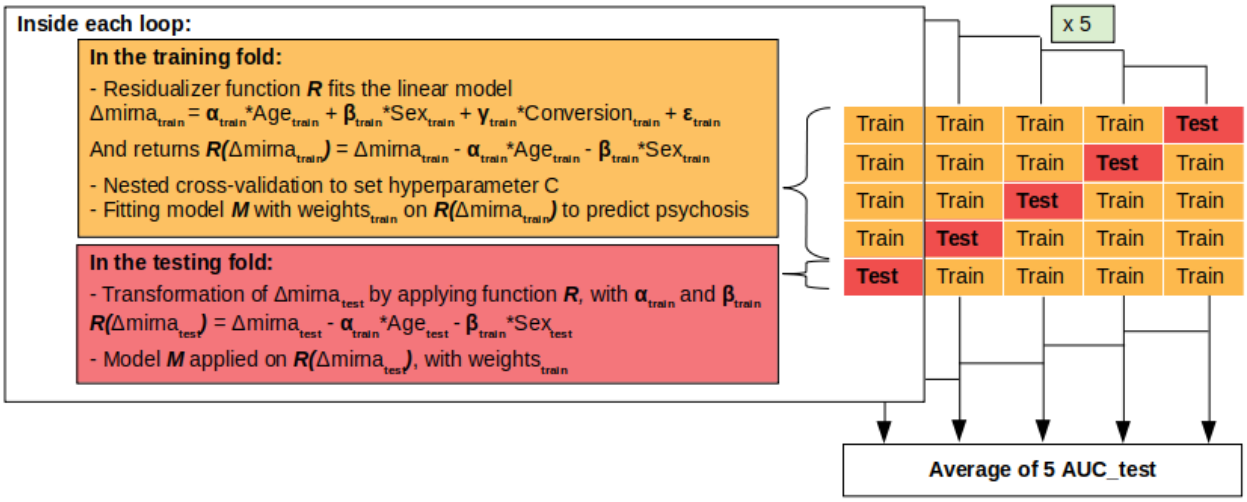

Supplementary Figure 3 - Repetition of the prediction under random permutation of labels to simulate the null hypothesis. We simulated the null hypothesis by randomly permuting converter and non-converter statuses among subjects, and repeated the machine-learning algorithm 10 000 times. We then computed how many times the average AUC was higher or equal to the observed one. The reported p-value was calculated as the ratio of this number to the total number of tests done.

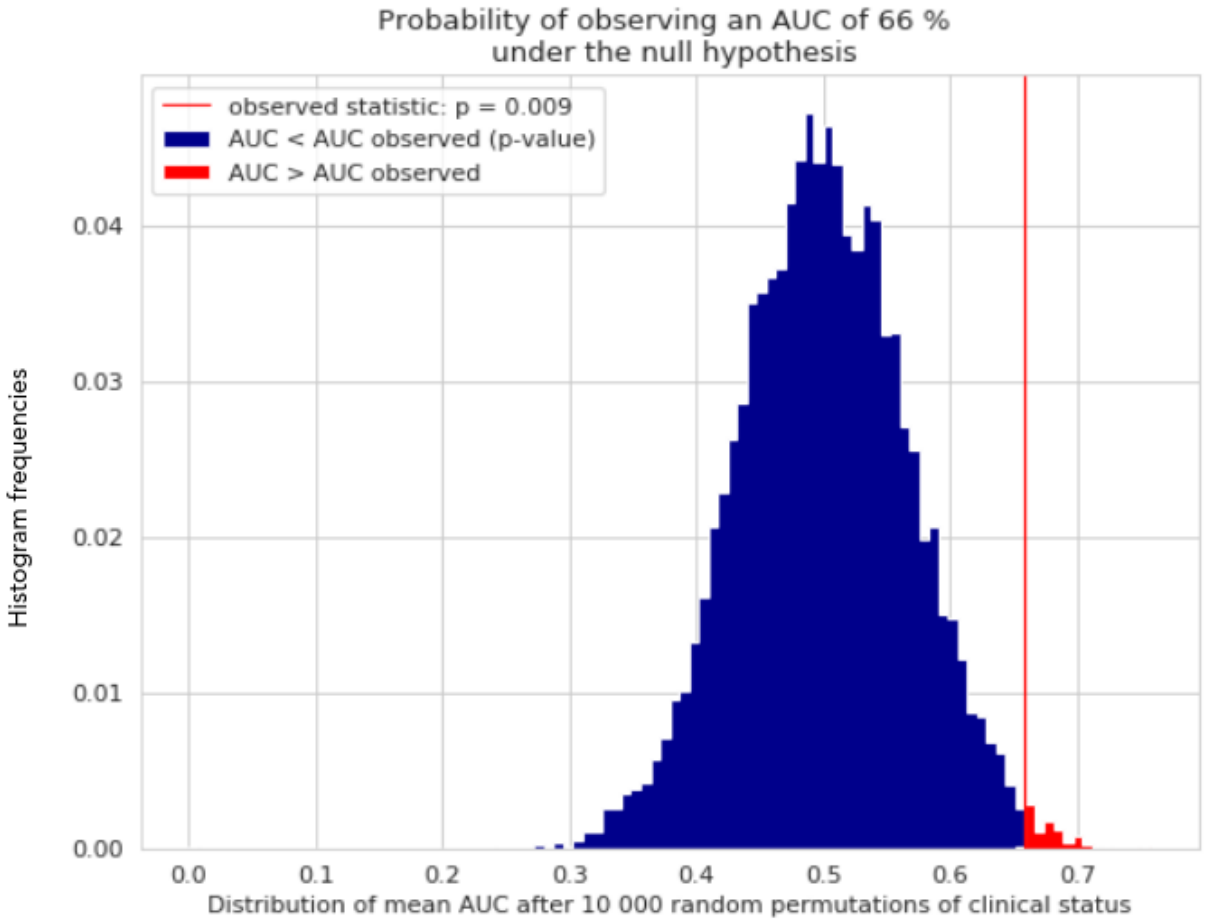

Supplementary Figure 4 - microRNAs most relevant for the classification algorithm. 207 Δmirnas have predicted weights with 95 % confidence intervals (colored bars) that do not include zero (vertical dashed line).

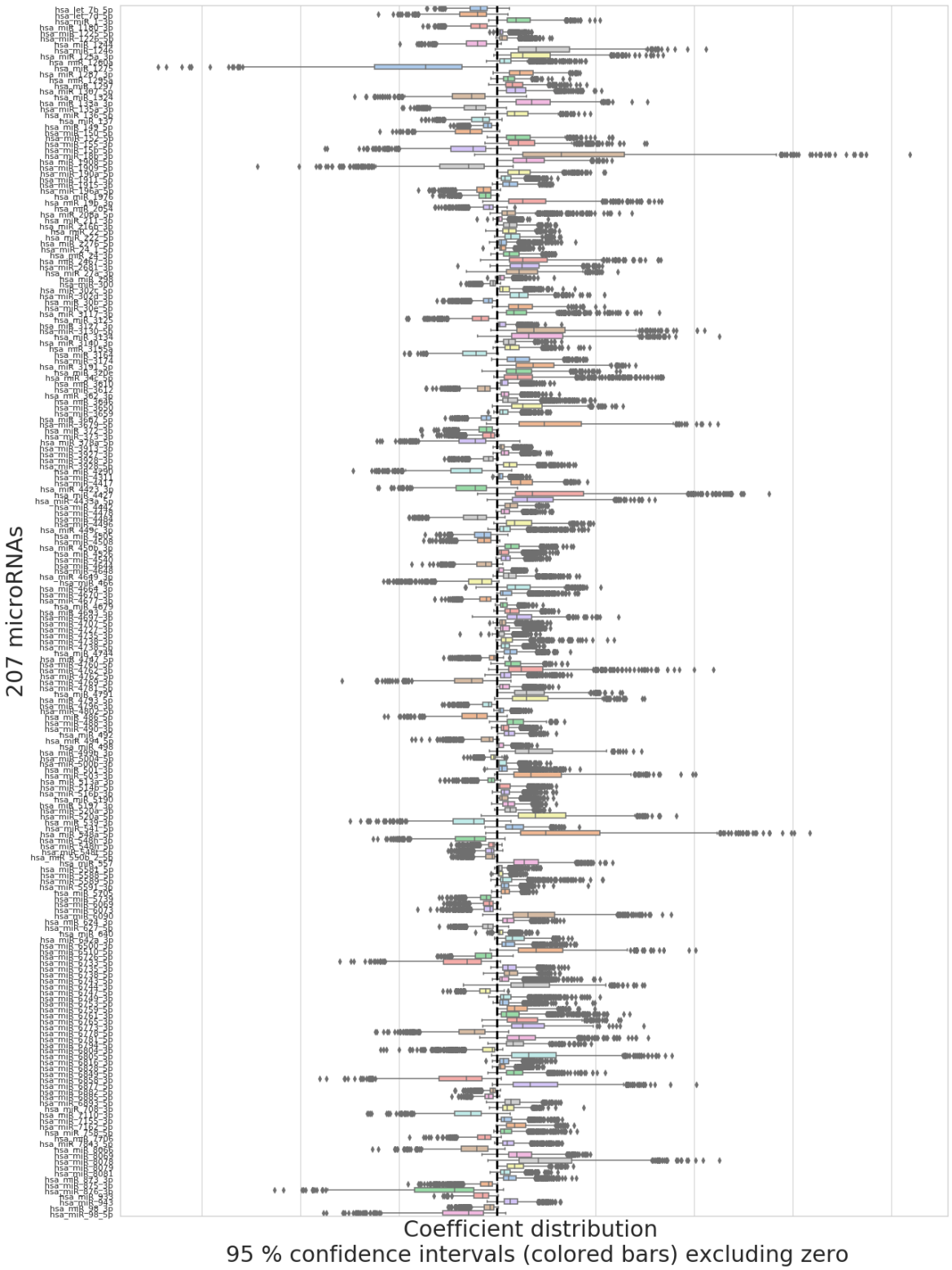

Supplementary Table 1 - Studies used as reference for the computation of chlorpromazine equivalents

Typical antipsychotic	Reference study	
Klorprotixene	(Kroken et al., 2009; Leucht et al., 2014)	[1,2]
Levomepromazine	(Kroken et al., 2009)	[1]
Trifluropromazine	(Davis, 1975)	[3]
Thioridazine	(Andreasen et al., 2010)	[4]
Dixyrazine	(Kroken et al., 2009)	[1]
Prochlorperazine	(Davis, 1975; Woods, 2005)	[3,5]
Perphenazine	(Andreasen et al., 2010)	[4]
Perphenazine decanoate	(Kroken et al., 2009)	[1]
Zuclopenthixol	(Kroken et al., 2009)	[1]
Zuclopenthixol decanoate	(Kroken et al., 2009)	[1]
Flupenthixol	(Kroken et al., 2009)	[1]
Flupenthixol decanoate	(Kroken et al., 2009)	[1]
Fluphenazine	(Andreasen et al., 2010)	[4]
Fluphenazine decanoate	(Andreasen et al., 2010)	[4]
Trifluoperazine	(Andreasen et al., 2010)	[4]
Acetophenazine	(Davis, 1975; Leucht et al., 2014)	[2,3]
Carphenazine	(Davis, 1975; Leucht et al., 2014)	[2,3]
Butaperazine	(Davis, 1975; Leucht et al., 2014)	[2,3]
Mesoridazine	(Davis, 1975; Leucht et al., 2014)	[2,3]

Piperacetazine	(Davis, 1975; Leucht et al., 2014)	[2,3]
Haloperidol	(Andreasen et al., 2010)	[4]
Haloperidol decanoate	(Andreasen et al., 2010)	[4]
Chlorprothixene	(Davis, 1975)	[3]
Thiothixene	(Andreasen et al., 2010)	[4]
Molindone	(Woods, 2005)	[5]
Prochlorperazine	(Leucht et al., 2014; Woods, 2005)	[2,5]
Atypical antipsychotics		
Risperidone	(Andreasen et al., 2010)	[4]
Risperidone action prolongée	(Kroken et al., 2009; Woods, 2005)	[1,5]
Olanzapine	(Andreasen et al., 2010)	[4]
Quetiapine	(Andreasen et al., 2010)	[4]
Ziprasidone	(Andreasen et al., 2010)	[4]
Aripiprazole	(Andreasen et al., 2010)	[4]
clozapine	(Andreasen et al., 2010)	[4]
Asenapine	(Leucht et al., 2014; Woods, 2005)	[2,5]
Iloperidone	(Leucht et al., 2014; Woods, 2005)	[2,5]
Lurasidone	(Leucht et al., 2014; Woods, 2005)	[2,5]
Paliperidone	(Leucht et al., 2014; Woods, 2005)	[2,5]
Sertindole	(Kroken et al., 2009; Leucht et al., 2014)	[1,2]
Amisulpride	(Bazire, 2007)	[6]
Sulpride	(Bazire, 2007)	[6]

Supplementary Table 2 - Differential microRNA expression, adjusted for age and sex.

ΔmiRNA	T-value	MaxT corrected p-value	Beta parameter	Unadjusted p-value	95% confidence interval
hsa_miR_3191_5p	3.56	0.001	1.24	0.001	[0.55, 1.94]
hsa_miR_150_5p	-3.14	0.023	-1.02	0.002	[-1.67, -0.37]
hsa_miR_1275	-2.85	0.078	-0.54	0.006	[-0.92, -0.16]
hsa_miR_6893_5p	2.78	0.098	1.25	0.007	[0.36, 2.15]
hsa_miR_4769_3p	-2.65	0.152	-0.82	0.01	[-1.44, -0.2]
hsa_miR_4442	2.6	0.183	0.58	0.011	[0.14, 1.02]
hsa_miR_3679_5p	2.3	0.383	0.47	0.024	[0.06, 0.88]
hsa_miR_4697_3p	2.08	0.587	0.55	0.041	[0.02, 1.08]
hsa_miR_499b_3p	2.06	0.597	0.13	0.043	[0.0, 0.26]
hsa_miR_18b_3p	2.06	0.597	0.27	0.043	[0.01, 0.53]
hsa_miR_6805_5p	1.99	0.661	0.59	0.05	[-0.0, 1.18]
hsa_miR_520a_5p	1.95	0.706	0.45	0.054	[-0.01, 0.91]
hsa_miR_4423_3p	-1.9	0.752	-0.24	0.062	[-0.5, 0.01]
hsa_miR_6877_5p	1.78	0.855	0.65	0.08	[-0.08, 1.38]
hsa_miR_557	1.71	0.895	0.32	0.092	[-0.05, 0.69]
hsa_miR_3134	1.61	0.941	0.18	0.113	[-0.04, 0.41]
hsa_miR_486_5p	-1.55	0.96	-0.59	0.124	[-1.34, 0.17]
hsa_miR_15b_5p	-1.51	0.968	-0.33	0.135	[-0.77, 0.11]
hsa_miR_125a_3p	1.47	0.975	0.51	0.144	[-0.18, 1.2]
hsa_miR_4433a_5p	1.31	0.993	0.33	0.195	[-0.17, 0.82]
hsa_miR_548h_3p	-1.29	0.994	-0.08	0.199	[-0.2, 0.04]
hsa_miR_1909_5p	-1.2	0.999	-0.48	0.232	[-1.26, 0.31]
hsa_miR_6090	0.13	1	0.05	0.898	[-0.77, 0.88]
hsa_miR_2681_3p	0.85	1	0.33	0.4	[-0.45, 1.12]
hsa_miR_98_5p	-0.87	1	-0.19	0.385	[-0.61, 0.24]

Supplementary Table 3 - Genes targeted by at least 3 microRNAs (see supplementary csv file for full mirDip output)

gene	Number of microRNAs targeting the gene
DYRK1A	7
IGF1R	7
C1orf21	6
RIMS3	6
CNOT6L	6
IKZF2	6
PAPPA	6
TPM3	5
EPB41L1	5
LCOR	5
BACH2	5
LPP	5
DCX	5
MECP2	5
CCND2	5
CELF2	5
SEMA6D	5
ONECUT2	5
ELMSAN1	5
VTI1A	5
AMOT	5
SLC1A2	5
SMAD2	5
CEP350	5
AEBP2	5
INSR	5
QKI	5
IGF1	5
NFAT5	5
DCAF8	4
PEG10	4
RSBN1	4

HMGA1	4
BCL11B	4
AGO1	4
KMT2A	4
BTBD9	4
PAG1	4
MAPK1IP1L	4
TRIM33	4
PHF20	4
PHC3	4
EIF4G2	4
FAM84B	4
ACVR2B	4
MYCL	4
CD47	4
ZNF148	4
MAN2A2	4
FZD4	4
OPA3	4
MNT	4
SLC4A7	4
WDR37	4
KHNYN	4
PSD3	4
SNX1	4
MOB3B	4
BNC2	4
PLPP6	4
GABRA4	4
RBFOX2	4
ABCC5	4
PCDH19	4
AMMECR1L	4
SYNJ1	4
RAB8B	4
RBM12	4
CDK6	4
SREK1IP1	4
DLGAP2	4

AFF2	4
AGO4	4
DCP2	4
MAPK9	4
NTRK2	4
TEX261	4
RNF38	4
CYB561D1	4
TGFBR1	4
FOXN3	4
DTNA	4
TEAD1	4
TP53INP1	4
TSC22D3	4
ERLIN2	4
BAZ2A	4
SSR1	4
ADAMTS5	4
AFF4	4
PHACTR2	4
HS2ST1	4
PIK3R1	4
NAV1	4
ATRN	4
NOTCH2	4
SNX27	4
SREK1	4
PGM2L1	4
HTR4	4
PDE4D	4
PAFAH1B1	4
RPS6KA3	4
UBFD1	4
HMGA2	4
CTDSPL2	4
UBN2	4
PDP1	4
E2F3	4
PURB	4

MAP3K9	4
MOB4	4
DCBLD2	4
ATXN1	4
RPS6KB1	4
CBL	4
NAA15	4
ARMC8	4
BRWD1	4
CPEB4	4
STEAP3	4
KCNC4	4
CMTM6	4
GATAD2B	4
ABHD2	4
SLC8A1	3
RAPGEFL1	3
CCSER2	3
TTC14	3
PRRC2C	3
SMARCD2	3
RNMT	3
PHF8	3
MBNL1	3
SH3TC2	3
PRRX1	3
NPR3	3
BPTF	3
DMRT2	3
EZH1	3
VEGFA	3
CAMK2G	3
RAB22A	3
AGPAT3	3
SLC12A5	3
PARD6B	3
PARP16	3
BMPR1A	3
SEMA3A	3

VAV2	3
DST	3
ADAMTS6	3
AKIRIN1	3
REPS2	3
ZC3HAV1	3
ANKRD12	3
CLOCK	3
RBFOX1	3
AKAP2	3
KCNMA1	3
RAB3IP	3
ACSL4	3
GAS7	3
KCNJ3	3
SEC22A	3
SMARCC1	3
EIF5A2	3
MTHFR	3
POM121C	3
SLC9A6	3
CHD9	3
ARHGAP20	3
NEXMIF	3
ZER1	3
C16orf72	3
FBXO21	3
ITPRIPL2	3
MIER3	3
CMTM4	3
TUBB	3
TBL1XR1	3
CAMSAP2	3
TAOK1	3
ASH1L	3
MIB1	3
C6orf120	3
ARHGAP5	3
CACNB2	3

BCL7A	3
WIPF2	3
RUNX1	3
GLCE	3
NUAK1	3
WDFY3	3
MAP3K3	3
RAPH1	3
PFKFB2	3
WDR26	3
JADE1	3
SYPL1	3
KPNA6	3
TMCC1	3
ARPP19	3
FAM208A	3
AKT2	3
TGOLN2	3
ATP2B1	3
NLGN1	3
MAMLD1	3
CREBZF	3
BZW1	3
ATG9A	3
DTX4	3
BSN	3
TOGARAM1	3
CHIC1	3
ATAD2B	3
ACOX1	3
YPEL2	3
MBD1	3
GJC1	3
GRPEL2	3
ZNF697	3
PPT2	3
ENAH	3
INO80D	3
TMC7	3

DNAJC16	3
CRTAP	3
KPNA1	3
BTF3L4	3
MEF2C	3
ITSN1	3
USP47	3
RTL3	3
SLC10A7	3
NRG1	3
CBX2	3
SUCO	3
POM121	3
IPO9	3
PITPNA	3
BBX	3
KLHL3	3
TRPS1	3
HBP1	3
MYO5A	3
EIF5	3
PTAR1	3
MASP1	3
NAB1	3
NOL4L	3
ZNRF2	3
POU2F1	3
NR4A3	3
AMOTL1	3
CYLD	3
B3GNT2	3
LIMD1	3
ZBTB33	3
NUP98	3
FOXP1	3
DVL3	3
MGA	3
ZFP91	3
TXLNG	3

ADAM19	3
ATXN7L3	3
CAST	3
COL4A3BP	3
SYT7	3
ATP2B2	3
ZHX3	3
PDLIM5	3
CALU	3
CADM2	3
PISD	3
PFN2	3
MAP2K4	3
P2RX7	3
YTHDF3	3
PPARA	3
PPP2R1A	3
PPP1R12B	3
WSB1	3
THRA	3
RB1	3
TNRC6A	3
OTUD4	3
ZKSCAN1	3
PRDM1	3
PLXNC1	3
ZNF609	3
ZIC1	3
TSPYL5	3
BEND4	3
ATP2B4	3
ATXN1L	3
TNPO1	3
PTPRD	3
RGS4	3
IRF2BP2	3
MBNL2	3
RICTOR	3
ISLR	3

ETNK1	3
HIPK2	3
VGLL3	3
ZCCHC3	3
ANK2	3
MAP4	3
RGS6	3
TMEM245	3
TNRC6B	3
CD84	3
BLOC1S6	3
LBH	3
NR2C2	3
BSDC1	3
UBE2W	3
SCN4B	3
KMT2D	3
ARHGEF9	3
NFASC	3
KIF2A	3
TENM2	3
XPO4	3
TMEM135	3
USP9X	3
UBE2J1	3
ZSCAN25	3
SP5	3
TET3	3
CELF1	3
SEC14L5	3
KMT5B	3
MYRIP	3
PLAGL2	3
PLA2G15	3
CPEB2	3
GAN	3
FGF7	3
WAPL	3
BTBD3	3

IGF2BP1	3
FOSL2	3
CD164	3
MAP3K13	3
POLD3	3
ZBTB5	3
CANX	3
DUSP3	3
DMD	3
ARNT	3
NMT1	3
LRP1B	3
PTPN3	3
FAM46C	3
YWHAZ	3
EPS15	3
MLLT10	3
KAZN	3
FRMD6	3
G3BP2	3
TSC22D2	3
SGK1	3
DCLK1	3
TAB3	3
ITGAV	3
PDCD4	3
MINOS1	3
SLC7A11	3
CREBRF	3
PPM1E	3
SSX2IP	3
ATRNL1	3
SLC7A6	3
FBN1	3
PURG	3
NLK	3
SLAIN2	3
KSR2	3
PGAP1	3

TMOD1	3
OPHN1	3
ASIC1	3
CCNJ	3
MYB	3
GPATCH8	3
SLC4A4	3
NAV2	3
VAPA	3
RCOR1	3
PRDM2	3
ARHGEF12	3
PTPRB	3
XIAP	3
MMP16	3
PTCH1	3
FAM60A	3
PRRG1	3
SRGAP2	3
RPP14	3
PDPR	3
MRPS25	3
CCNT2	3
LHX6	3
PAPOLG	3
EDA	3
GANAB	3
CPD	3
PBX3	3
DYNC1LI2	3
STX3	3
PLAG1	3
JADE3	3
RFFL	3
PAFAH2	3
ACVR2A	3
OSBPL3	3
GATM	3
FNDC3B	3

TMEM55A	3
DESI2	3
KIF1B	3
ZFAND5	3
CTDSPL	3
ULK2	3
CYB5B	3
IGF2BP2	3
STK39	3
ATP6V1A	3
MTMR4	3
GALNT1	3
CLCN5	3
RAB14	3
BDNF	3
UTP15	3

Supplementary references :

1. Kroken, R. A., Johnsen, E., Ruud, T., Wentzel-Larsen, T. & Jørgensen, H. A. Treatment of schizophrenia with antipsychotics in Norwegian emergency wards, a cross-sectional national study. BMC Psychiatry 9, 24 (2009).

2. Leucht, S. et al. Dose equivalents for second-generation antipsychotics: the minimum effective dose method. Schizophr. Bull. 40, 314–326 (2014).

3. Davis, J. M. Dose equivalence of the antipsychotic drugs. in Catecholamines and Schizophrenia 65–73 (Elsevier, 1975).

4. Andreasen, N. C., Pressler, M., Nopoulos, P., Miller, D. & Ho, B.-C. Antipsychotic dose equivalents and dose-years: a standardized method for comparing exposure to different drugs. Biol. Psychiatry 67, 255–262 (2010).

5. Woods, S. W. Calculation of CPZ Equivalents. at <www.scottwilliamwoods.com/files/Equivtext.doc> (2005).

6. Bazire, S. Psychotropic Drug Directory, Maudsley Guideline. (2007).